

RESEARCH ARTICLE

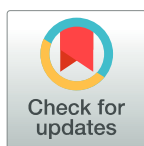
Rhodnius prolixus: Identification of missing components of the IMD immune signaling pathway and functional characterization of its role in eliminating bacteria

Nicolas Salcedo-Porras¹✉*, Alessandra Guarneri²✉, Pedro L. Oliveira³✉, Carl Lowenberger¹✉

1 Centre for Cell Biology, Development, and Disease, Department of Biological Sciences, Simon Fraser University, Burnaby, British Columbia, Canada, 2 Instituto René Rachou, Avenida Augusto de Lima, Belo Horizonte, Minas Gerais, Brazil, 3 Instituto de Bioquímica Médica, Universidade Federal do Rio de Janeiro, CCS, Ilha do Fundão, Rio de Janeiro, Brazil

✉ These authors contributed equally to this work.

* nicolas_salcedo@sfu.ca



OPEN ACCESS

Citation: Salcedo-Porras N, Guarneri A, Oliveira PL, Lowenberger C (2019) *Rhodnius prolixus*: Identification of missing components of the IMD immune signaling pathway and functional characterization of its role in eliminating bacteria. PLoS ONE 14(4): e0214794. <https://doi.org/10.1371/journal.pone.0214794>

Editor: Daniel Doucet, Natural Resources Canada, CANADA

Received: December 19, 2018

Accepted: March 20, 2019

Published: April 3, 2019

Copyright: ©2019 Salcedo-Porras et al. This is an open access article distributed under the terms of the [Creative Commons Attribution License](https://creativecommons.org/licenses/by/4.0/), which permits unrestricted use, distribution, and reproduction in any medium, provided the original author and source are credited.

Data Availability Statement: All relevant data are within the manuscript and its Supporting Information files.

Funding: This work was supported by NSERC Discovery grant to CL (RGPIN261940), www.nserc-crsng.gc.ca; MITACS Globalink Research Award to NSP (IT08650), <https://www.mitacs.ca/en/programs/globalink/globalink-research-award>. The funders had no role in study design, data

Abstract

The innate immune system in insects is regulated by specific signalling pathways. Most immune related pathways were identified and characterized in holometabolous insects such as *Drosophila melanogaster*, and it was assumed they would be highly conserved in all insects. The hemimetabolous insect, *Rhodnius prolixus*, has served as a model to study basic insect physiology, but also is a major vector of the human parasite, *Trypanosoma cruzi*, that causes 10,000 deaths annually. The publication of the *R. prolixus* genome revealed that one of the main immune pathways, the Immune-deficiency pathway (IMD), was incomplete and probably non-functional, an observation shared with other hemimetabolous insects including the pea aphid (*Acyrtosiphon pisum*) and the bedbug (*Cimex lectularius*). It was proposed that the IMD pathway is inactive in *R. prolixus* as an adaptation to prevent eliminating beneficial symbiont gut bacteria. We used bioinformatic analyses based on reciprocal BLAST and HMM-profile searches to find orthologs for most of the “missing” elements of the IMD pathway and provide data that these are regulated in response to infection with Gram-negative bacteria. We used RNAi strategies to demonstrate the role of the IMD pathway in regulating the expression of specific antimicrobial peptides (AMPs) in the fat body of *R. prolixus*. The data indicate that the IMD pathway is present and active in *R. prolixus*, which opens up new avenues of research on *R. prolixus*-*T. cruzi* interactions.

Introduction

The immune system of arthropods relies exclusively on an innate response triggered by the detection of conserved Pathogen Associated Molecular Patterns (PAMPs) found on the surface of microorganisms [1]. In arthropods, the elimination of opportunistic pathogens, the

collection and analysis, decision to publish, or preparation of the manuscript.

Competing interests: The authors have declared that no competing interests exist.

regulation of beneficial symbionts, and the immune response to eukaryotic parasites is orchestrated by a handful of well conserved molecular pathways such as the Toll pathway, the immune deficiency (IMD) pathway, the JAK-STAT pathway, and the RNAi pathway [2–5]. Each of these pathways has been associated, historically, with the control of subgroups of pathogens. Traditionally the Toll pathway has been considered to be induced by Gram-positive bacteria and fungi, the IMD pathway by Gram-negative bacteria, and JAK-STAT and RNAi pathways by viruses, although we now know that there is cross talk among the various pathways [6–9]. Most of our understanding of immune responses has been derived from dipteran models such as *Aedes aegypti* and *Drosophila melanogaster* and it has been assumed that these findings apply universally to all other arthropods. Current evidence from ticks, chelicerates, hemipterans, and lice describe a deviation from the idea of complete conservation of immune responses and pathways, highlighting the need to study basic immune responses in disparate species [9–15].

One of the first organisms used to study basic concepts of insect physiology was the hematophagous triatomine bug, *Rhodnius prolixus* [16–18]. This insect also is a principal vector of *Trypanosoma cruzi*, which causes Chagas disease in humans, killing ~12,000 people annually and affecting 6–10 million people worldwide [19,20]. Triatomines ingest *T. cruzi* trypomastigotes when they feed on infected vertebrates. In contrast to other vector borne parasites that invade the insect body cavity and replicate in salivary glands, *T. cruzi* develops and replicates solely within the gastrointestinal (GI) tract of the insect, and infective forms of the parasite are released and transmitted with the feces as the insect feeds. If this parasite invades the body cavity of the insect vector it is promptly eliminated by elements of the innate immune system [21,22]. Moreover, *R. prolixus* is the only triatomine to have had its genome sequenced and published, which makes it an ideal model to investigate innate immune responses in a non-dipteran blood feeding insect vector.

The molecular interactions between trypanosomes, the vector's innate immune system, and the obligate endosymbiotic bacterial symbionts of *R. prolixus* have received increased attention over the last decade. The principal symbiotic bacterium in the microbiome of *R. prolixus* is the Gram-positive bacterium *Rhodococcus rhodnii*, found mainly in the anterior midgut (AM) region of the insect. Within 48 hours of ingesting a blood meal, the population of *R. rhodnii* increases 10,000 times [23,24]. Concomitantly, the population of *T. cruzi* ingested with a blood meal shows a 90% reduction in the AM within 24 hours [25]. Although parasite reduction is independent of the bacterial population [26], *T. cruzi* infection induces the expression of immune factors including antimicrobial peptides (AMPs), nitric oxide, phenoloxidase, lectins, and protease inhibitors [27–29], suggesting a direct interaction or competition for resources [24,30,31].

Infections with trypanosomes and bacteria trigger a tissue specific immune response in *R. prolixus*; experimental infection with *T. cruzi* and *Trypanosoma rangeli* modulate the expression of AMPs depending on the infection timepoint, tissue (Fat Body (FB) or Midgut (MG)), the trypanosome strain, and the dominant microbiome [21,30–33]. In general, *T. rangeli* infections reduce the expression of Lysozyme-B (Lys-B) and Prolixicin, and induce the expression of Defensin-C (Def-C) in the MG; while infections with the *T. cruzi* dm28c strain induces Def-C and Prolixicin in the MG [31,32]. Insects fed on blood infected with Gram-positive bacteria showed higher transcription of Def-A, Def-B, Prolixicin, Lys-A in the AM; and of Def-C in the Posterior midgut (PM); and reduced transcription of Prolixicin in the PM 24h after feeding [34]. Feeding with blood containing Gram-negative bacteria induces the transcription of Def-B and Def-C in the AM; of Lys-A in the PM; and reduced transcription of Prolixicin in the PM, and Lys-B in the AM 24h after feeding [34]. Similar immune responses have been reported in *R. prolixus* injected intrathoracically with a

combination of Gram-positive and Gram-negative bacteria [32,33,35,36]. Within 24h of the infection, Def-A, Def-B, and Lys-A transcripts increase in the MG, while Def-A, Def-B, Prolixin, and Lys-B are induced in the FB. These results confirm an overall and robust activation and regulation of the innate immune system of *R. prolixus*, but the pattern of AMP expression does not follow the traditional separation of Toll and IMD regulated expression.

When the genome of *R. prolixus* was published several elements of the IMD pathway were reported as “missing”, and the authors questioned whether this pathway was functional in this insect [37]. Similarly, a reduced IMD pathway was reported in the genomes of other hemimetabolous insects including the pea aphid (*Acyrtosiphon pisum*) [13], the bedbug (*Cimex lectularius*) [38] and the head louse (*Pediculus humanus*) [39]. These researchers proposed that a reduced or inactive IMD pathway was an adaptation to prevent harming the obligate beneficial bacterial symbionts [13,37].

The *R. prolixus* genome was reported to lack genes encoding immune deficiency (IMD), Fas-associated Death Domain (FADD), death-related ced-3/Nedd2-like (DREDD), the I- κ B kinase β (IKK β), Cylindromatosis (CYLD), Caspar (a negative regulator of the IMD pathway), and the E2 ubiquitination complex (Effete, Uev1A, and Bendless). Despite the apparent absence of these highly conserved members of the IMD pathway, transcriptome studies have reported the expression of transcripts of Relish and a potential Caspar ortholog [40], and gene expression data on AMPs putatively regulated by the IMD pathway are expressed [32,36]. Whether the IMD pathway functions through novel proteins linking existing IMD pathway components, or through a non-canonical pathway, is unknown. Using a combination of bioinformatics and wet bench studies, we have identified most of the “missing” orthologs of the IMD pathway in *R. prolixus*. In addition, we have silenced Relish to demonstrate that the IMD pathway in *R. prolixus* is similar to that of most holometabolous insects. These data indicate that the IMD pathway is present and inducible in *R. prolixus*, and that it is activated preferentially by Gram-negative bacteria.

Materials and methods

Ethics statement

All animal care and experimental protocols were conducted following the guidelines of the institutional care and use committee (Committee for Evaluation of Animal Use for Research from the Federal University of Rio de Janeiro), which are based on the National Institutes of Health Guide for the Care and Use of Laboratory Animals (ISBN 0-309-05377-3). The protocols were approved by the Committee for Evaluation of Animal Use for Research (CAUAP) from the Federal University of Rio de Janeiro, under registry number 115/13. Technicians dedicated to the animal facility at the Institute of Medical Biochemistry (Federal University of Rio de Janeiro) carried out all aspects related to rabbit husbandry under strict guidelines to ensure careful and consistent handling of the animals.

Insect rearing

A colony of *R. prolixus* is maintained in the insectary of the Institute of Medical Biochemistry at the Federal University of Rio de Janeiro. These insects were fed on live rabbits at three-week intervals and maintained at 28°C and 80–90% relative humidity under a photoperiod of 12h of light and 12h of dark. Recently moulted (1–2 days) fifth instar nymphs were used in the experiments and were maintained under the standard rearing conditions described.

IMD pathway homolog search

A combination of strategies was used to identify candidate orthologs of “missing” IMD pathway genes in *R. prolixus*. We used multiple reciprocal BLAST searches and hidden Markov models (HMM) to create a non-redundant list of candidate orthologs in *R. prolixus* [12]. We built an IMD pathway genes database gathering sequences from Flybase, III-DB, ORTHO-MCL, Insect-base, I5k, Immuno-DB, and Beebase [41–48].

BLASTn, BLASTp, and tBLASTx searches were performed using amino acid and nucleotide sequences from the IMD pathway genes database as queries against the *R. prolixus* protein gene set-C3.1 and against published transcriptomes [40,49]. Matches with significant similarity (e-values < 1×10^{-5} , identity > 20%, and query coverage > 50%) were used in reciprocal BLAST searches against a data set comprising 142 arthropod gene-sets using information from Insect-base, IK-5, Flybase, Ensemble genomes, and NCBI transcriptome projects. Candidate orthologs were assessed for conserved protein domain architecture using NCBI Conserved Domain Search and compared with canonical IMD protein domain architecture.

Subsequently, HMM profile searches were performed by building multiple alignments of candidate IMD pathway ortholog proteins from various arthropods. Sequences were selected to avoid taxonomic bias, using crustaceans, arachnids, hemimetabolous and holometabolous insects. The accession numbers for the full sequences can be found in Supplementary File 1 (S1 File) that was used in the phylogenetic analyses. Multiple alignments were built using MUSCLE algorithm and manually edited on MEGA 7.0 software [50,51]. The HMM profiles were built with HMMER 3.1 using default settings and used to search the *R. prolixus* protein gene set-C3.1 and protein translated transcriptomes using default settings. HMM profile ortholog sequences were retrieved from KEGG, I5K, Ensemble, and NCBI genome and transcriptome sequencing projects [47,52,53].

PCR and sequencing of IMD pathway homolog candidates

Rhodnius prolixus candidate gene sequences identified using these procedures were retrieved from Vector Base and transcriptome assemblages [40,49,54]. Primers were designed for use in PCR to confirm the transcription of these genes using cDNA templates derived from fat body tissues from immune challenged insects [36]. All reactions used the ABM 2x PCR Taq Master-mix (ABM, Richmond, Canada). Sequences were deposited in GenBank under accession numbers MH484616 to MH484621. Sequences, PCR conditions, and primers used are listed in Supplementary File 1 (S1 File).

Phylogenetic analysis

Multiple protein alignments with complete sequences or conserved domain sequences were made for “missing” members of the IMD pathway: FADD, DREDD, IAP2, Effete, Bendless, Uev1a, Caspar, CYLD, and IKK β . Representative arthropod sequences were used if they had been part of other immune studies, had been functionally characterized, or had been manually annotated. Sequences that only had automatic annotations were not used to construct these trees. Human tumour necrosis factor receptor network homologs to IMD pathway genes were used as outgroup sequences. Multiple alignments were made using MUSCLE default parameters in the program MEGA 7.0 [51] (S1 File). Maximum Likelihood analyses were done using IQ-TREE. Best-fit models for each gene alignment were selected based on the Bayesian Information Criterion (BIC). Branch support was assessed by 1000 ultrafast bootstrap replicates and with the Sh-aLTR test.

dsRNA target selection and synthesis of double-stranded RNA

We performed a selective analysis of rpRelish sequences to reduce the off-target silencing caused during dsRNA injections. The rpRelish cDNA sequence (Genbank sequence KP129556.1) was divided into 19 nucleotide fragments and used as queries with BLASTn against the *R. prolixus* transcripts-C3.1 data-set retrieved from Vectorbase. Any hits against genes other than rpRelish larger than 17 nucleotides, > 90% identity, and < 3 gaps were mapped to the rpRelish cDNA and a region with the least number of potential off-target silencing fragments was selected to amplify a 564 bp fragment. For a silencing control, the *Arabidopsis thaliana* AINTEGUMENTA (ANT) gene was subjected to the same analysis and primers were designed to amplify a 516 bp fragment. All primers are listed in [S2 Table \(S2 Table\)](#). PCR used cDNA templates from previous experiments done in our research group and were derived from the fat body of insects challenged with *Escherichia coli* and *Micrococcus luteus* [36] and the products were ethanol precipitated and sequenced. The same primers with an added 5' incorporated T7 polymerase binding site were used to generate the template required to generate dsRNA. These PCR products were ethanol precipitated and sequenced, and then were used as templates to synthesize double-stranded RNA (dsRNA) as previously described [55]. dsRNA synthesis products were ethanol precipitated, visualized on 1% agarose gel, and quantified on a Nanodrop 1000 spectrophotometer v. 3.7 (Thermo Fisher Scientific).

RNAi experiments

Intrathoracic injections of dsRNA generated from *R. prolixus* Relish, or the ANT gene, were performed on 5th instar insects 1–2 days after moulting. dsRNA was resuspended in 0.9% sterile saline solution and insects were injected with 1 μ L containing 2.5 μ g of dsRNA using a 10 μ L Hamilton syringe.

Immune challenge

Four days after dsRNA injections, insects were immune challenged by the intrathoracic injection of Gram-negative bacteria (*Enterobacter cloacae*) or Gram-positive bacteria (*Staphylococcus aureus*). Glycerol stocks from these bacteria were grown in Lysogeny Broth (LB) overnight at 200 rpm and 37° C. The liquid cultures were centrifuged, and the pellet was washed 2 times in PBS (137 mM NaCl; 2.7 mM KCl; 10 mM sodium phosphate at pH 7.2). The concentration of bacteria was calculated by spectrometry at 600nm on a Shimadzu UV-2550 spectrophotometer. Insects were injected with 2 μ L (~10⁸ total bacteria) using a 10 μ L Hamilton syringe. Control insects were injected with 2 μ L of sterile PBS. Insects were dissected in PBS and fat body tissues were extracted 8 hours after the immune challenge. Each treatment had 5 replicates of 3 pooled fat bodies.

Tissue isolation, RNA extraction, and cDNA synthesis

Total RNA from dissected FB tissues was extracted using TRIzol reagent (Invitrogen, Carlsbad, CA, US) following manufacturer's recommendations. DNase treatment was performed with TURBO DNA-free Kit (Ambion). The samples were quantified on a Nanodrop 1000 spectrophotometer v. 3.7 (Thermo Fisher Scientific). First strand cDNA synthesis was performed in 20 μ L reactions containing 2.0 μ g total RNA using an oligo dT primer (MG) with the One-Script cDNA Synthesis Kit (ABM, Canada) and an extension time of 50 minutes. The subsequent cDNA was diluted 1:50 with DEPC water.

Quantitative real-time PCR

Quantitative real-time PCR (qPCR) was used to assess *rpRelish* silencing on the expression of selected AMPs known to have a differential expression in fat body or hemocoel after infection with bacteria or protozoans. Primers were designed, or retrieved from the literature, for: α -Tubulin, *rpRelish*, *rpCaspar*, *Prolixicin*, *Lysozyme-B*, *Defensin-A*, and *Defensin-C* (S3 Table). All reactions contained 4.4 μ L of cDNA, 300mM of each primer, and 5 μ L of PerfeCTa SYBR Green Super Mix (Quanta Biosciences, Gaithersburg, MD, US) in a final volume of 10 μ L. qPCR was performed on a LightCycler96 thermal cycler (Roche diagnostics, Mannheim, Germany). The qPCR conditions used were: 95°C: 3 min, 40 cycles of 95°C: 15 s and 60°C: 30 s, followed by a melt curve analysis to confirm the specificity of the reaction. No-template controls were included with each primer set to verify the absence of exogenous DNA and primer-dimers. Relative differences in transcripts levels were calculated using the $2^{-\Delta\Delta Ct}$ method [56–58] with α -Tubulin (RPRC003295) as the reference gene. PCR efficiencies (E) for each primer were determined using the slope of a linear regression mode.

Statistical analysis

All treatments were tested for normality using the Shapiro-Wilk normality test and compared using the unpaired Student's T-test or Mann Whitney U Test. Calculations and graphs were made using R 3.0.14 and JMP 13.1. P-values lower than 0.05 were considered as evidence for difference between treatments. Relative transcript levels were expressed as means with whiskers representing \pm SEM.

Results

Rhodnius prolixus IMD pathway orthologs

IMD pathway candidate orthologs were found using reciprocal BLAST and HMM-profile searches (Table 1). *rpFADD* (RPRC013858), *rpDREDD* (GECK01002741.1), *rpCaspar* (RPRC001459), *rpIKK β* (GECK01053880.1), *rpIAP2* (RPRC007068), *rpEffete* (RPRC005317), *rpUev1a* (RPRC011375), *rpBendless* (RPRC011790), and *rpCYLD* (GECK01020525.1) orthologs were found using both search strategies. We did not find candidate orthologs for IMD or Kenny. We confirmed that all orthologs were transcribed using PCR amplification of cDNAs generated from fat body tissues of immune activated insects or by finding their transcripts in published transcriptomes [40,49]. Two orthologs, *rpDREDD* and *rpIKK β* , not currently annotated in the *R. prolixus* genome could not be amplified using PCR, but were found in published transcriptomes. *rpCYLD* is partially annotated in the *R. prolixus* genome (RPRC014665) but spans 3 contigs that are assembled in opposing directions, breaking the gene into 3 unlinked fragments. Newly identified putative *R. prolixus* orthologs of each gene contain regions that resemble highly conserved architecture and domains of known IMD pathway proteins in other organisms (Figs 1–5) based on sequence alignments (S1 File).

To evaluate the evolutionary relationships of *R. prolixus* IMD pathway orthologs ML phylogenetic trees with arthropod proteins sequences were built. We included all IMD pathway orthologs found in hemipterans even though no IMD pathway genes have been characterized functionally in this group with the exception of *Relish* in *R. prolixus* [37]. In trees for *FADD*, *DREDD*, *Caspar*, *IKK β* , *IAP2*, and *CYLD*, non-insect arthropods are basal to insects and holometabolous and hemimetabolous insect orthologs are found in mixed clades (Figs 1–3 and Fig 5). *Caspar* and *IKK β* trees share a similar topology with most hemimetabolous insects as a sister clade to all holometabolous insects (Fig 2B and Fig 3A). *Uev1a*, *Effete*, and *Bendless* orthologs are contained in a single clade separate from the other protein clades. These proteins have

Table 1. *Rhodnius prolixus* IMD pathway orthologs, BLASTp search best hit results, and hidden Markov model profile search results.

R. prolixus ortholog and accession numbers	BLASTp search results			HMM profile search results
	Best-match	Protein name	e-value	e-value
FADD (RPRC013858, GECK01061114.1, MH484617)	<i>Aethina tumida</i>	FADD	1.0x10 ⁻⁸	1.8x10 ⁻¹⁵
DREDD (GECK01002741.1)	<i>Oncopeltus fasciatus fasciatus</i>	DREDD	6.0x10 ⁻⁴⁰	1.1x10 ⁻⁸⁴
CASPAR (RPRC001459, GECK01051516.1 MH484616)	<i>Locusta migratoria</i>	CASPAR	3.0x10 ⁻¹⁶⁹	7.8x10 ⁻²⁰¹
IKKβ (GECK01053880.1)	<i>Cimex lectularius</i>	IKKβ	3.0x10 ⁻¹⁶¹	3.8x10 ⁻¹⁶⁵
IAP2 (RPRC007068, GECK01058463.1, MH484621)	<i>Oncopeltus fasciatus</i>	IAP2	0.0	1.4x10 ⁻¹⁶⁸
Effete (RPRC005317, GECK01025104.1, MH484619)	<i>Anoplophora glabripennis</i>	Effete	3.0x10 ⁻¹⁰⁵	3.1x10 ⁻¹⁰¹
Uev1a (RPRC011375, GECK01033612.1, MH484620)	<i>Cimex lectularius</i>	Uev1a	2.0x10 ⁻⁹⁸	1.2x10 ⁻⁸⁵
Bendless (RPRC011790, GECK01105599.1, MH484618)	<i>Halyomorpha halys</i>	Bendless	1.0x10 ⁻¹⁰⁵	7.6x10 ⁻⁹⁶
CYLD (GECK01020525.1)	<i>Dystrichothorax novaeangliae</i>	CYLD	0.0	0.0

BLASTp searches used protein sequences against a custom arthropod database. BLASTp Identity percentage and query coverage are over 25% and 73% respectively, for the results shown. HMM protein profile searches were done against a database comprised of the *R. prolixus* gene set version 3.1 and selected sequences from transcriptomes. The sequences used for the BLAST searches were from Vector-Base (sequences starting with RPRC), antennal transcriptome [49] (sequences starting with GECK), or sequences generated in this study (Sequences starting with MH). If the sequences were different among sources then the transcriptome sequences were used in the BLAST searches.

<https://doi.org/10.1371/journal.pone.0214794.t001>

almost identical, and extremely conserved, sequences that does not allow a determination of their evolutionary relationships (Fig 4).

Fas-associated protein with death domain ortholog (FADD)

Rhodnius prolixus FADD (rpFADD) has a Death Domain shared with *Drosophila melanogaster* and *Homo sapiens* orthologs. The Death Effector Domain present in most orthologs was not detected in *R. prolixus*. However, a similar architecture was reported for FADD found in other hemimetabolous insects, most hymenopterans insects, fleas, and mosquitoes. rpFADD clusters with other hemimetabolous FADD orthologs and are in a common clade with hymenopterans and coleopterans.

Death-related oed-3/Nedd2-like protein ortholog (DREDD)

Rhodnius prolixus DREDD (rpDREDD) has a caspase domain that is conserved in all DREDD orthologs including the human ortholog. ML trees show rpDREDD and hemipteran DREDD orthologs in a clade sister to the majority of insects (Fig 2A). Interestingly, hemipterans and hymenopterans form separate clades from other hemimetabolous and holometabolous insects, respectively.

FAF1 ortholog (CASPAR)

Rhodnius prolixus CASPAR (rpCASPAR) has a UAS family FAS-associated factor 1 domain and a UBL superfamily domain similar to *D. melanogaster* CASPAR. This protein is shorter than other orthologs and lacks a UBA-FAF1 and UBL domain present in other (but not all) orthologs. The ML-tree of this gene shows rpCASPAR in a clade with other hemipteran and paraneopteran insects (Fig 2B). Interestingly, aphid homologs are in a separate clade that is basal to other insects.

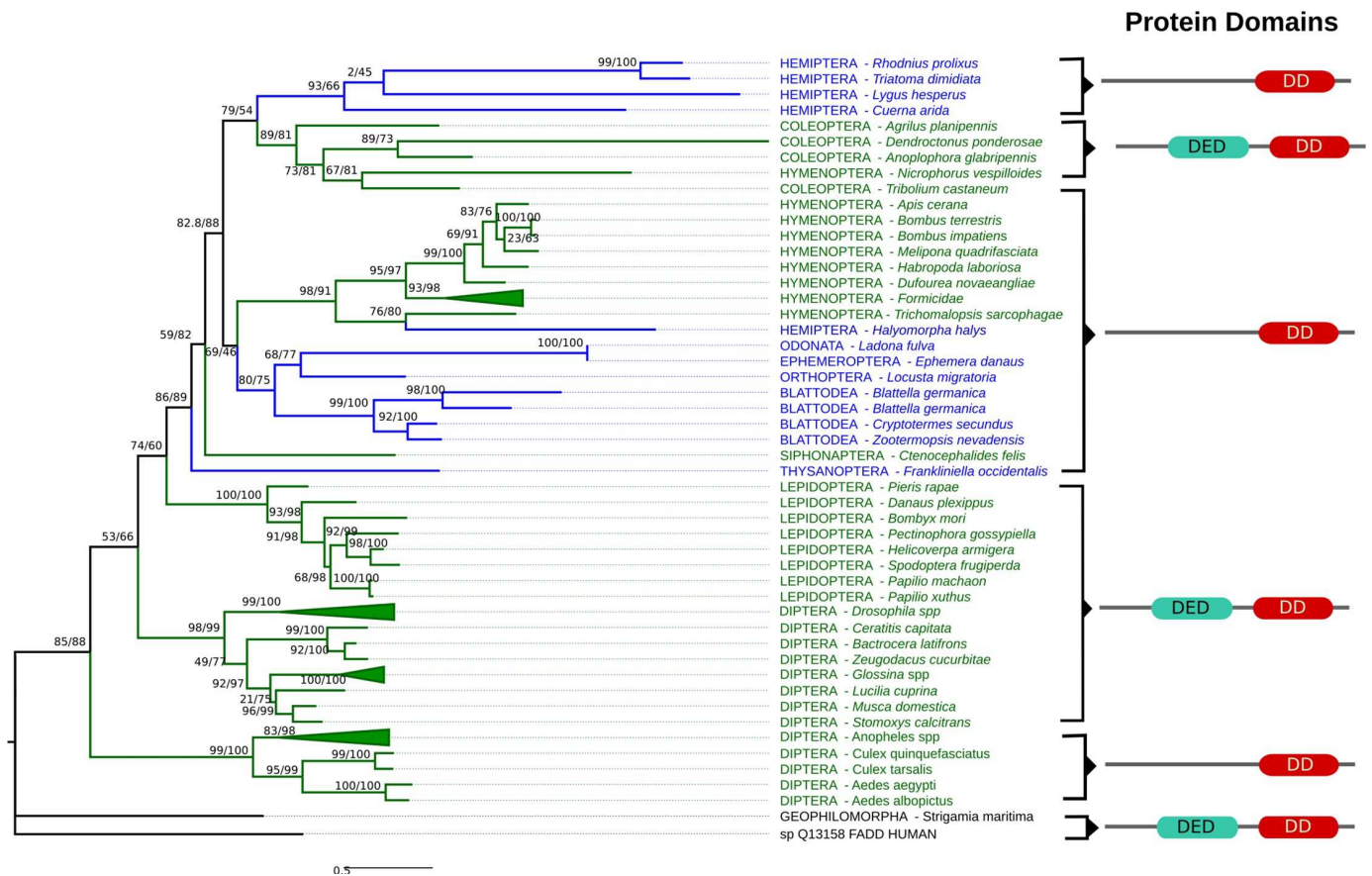


Fig 1. FADD Maximum likelihood trees in selected arthropods. rpFADD forms a common clade with other hemimetabolous insects, coleopterans and hymenopterans. Similar to FADD reported in mosquitoes, rpFADD only has a Death Domain (DD). The Death Effector Domain (DED) present in other orthologs was not detected in rpFADD or mosquitoes. Formicidae, Drosophila and Anophelidae clades are collapsed. The human FADD ortholog was used as the outgroup.

<https://doi.org/10.1371/journal.pone.0214794.g001>

The inhibitor of nuclear factor kappa-β kinase ortholog (IKKβ)

The IKKβ ortholog in *R. prolixus* (rplIKKβ) has a catalytic Serine/Threonine kinase, Inhibitor of Nuclear Factor-Kappa B Kinase beta domain present on all IKKβ orthologs. The ML phylogenetic tree for these proteins shows holometabolous and hemimetabolous insects in separate clades (Fig 3A). rplIKKβ is within the latter clade. The human louse *P. humanus* is the only hemimetabolous insect that deviates from this pattern, forming a basal clade to these two clades.

Inhibitor of apoptosis 2 ortholog (IAP2)

The IAP2 ortholog in *R. prolixus* (rplIAP2) has the same domain architecture found in *D. melanogaster* IAP2 protein. rplIAP2 has 3 BIR domains, 1 UBA domain, and 1 RING-HC domain. The ML tree of this protein shows a clade with all insect IAP2 orthologs (Fig 3B). Hemimetabolous and holometabolous orders form mixed clades that have strong branch support only at the order level. rplIAP2 is in a clade with all other hemipterans.

Effete, Bendless, and Uev1a orthologs

Effete, Bendless, and Uev1a are ubiquitin conjugating enzymes that share a UBC domain. Reciprocal BLAST searches indicate that RPRC005317, RPRC011375, and RPRC011790 could

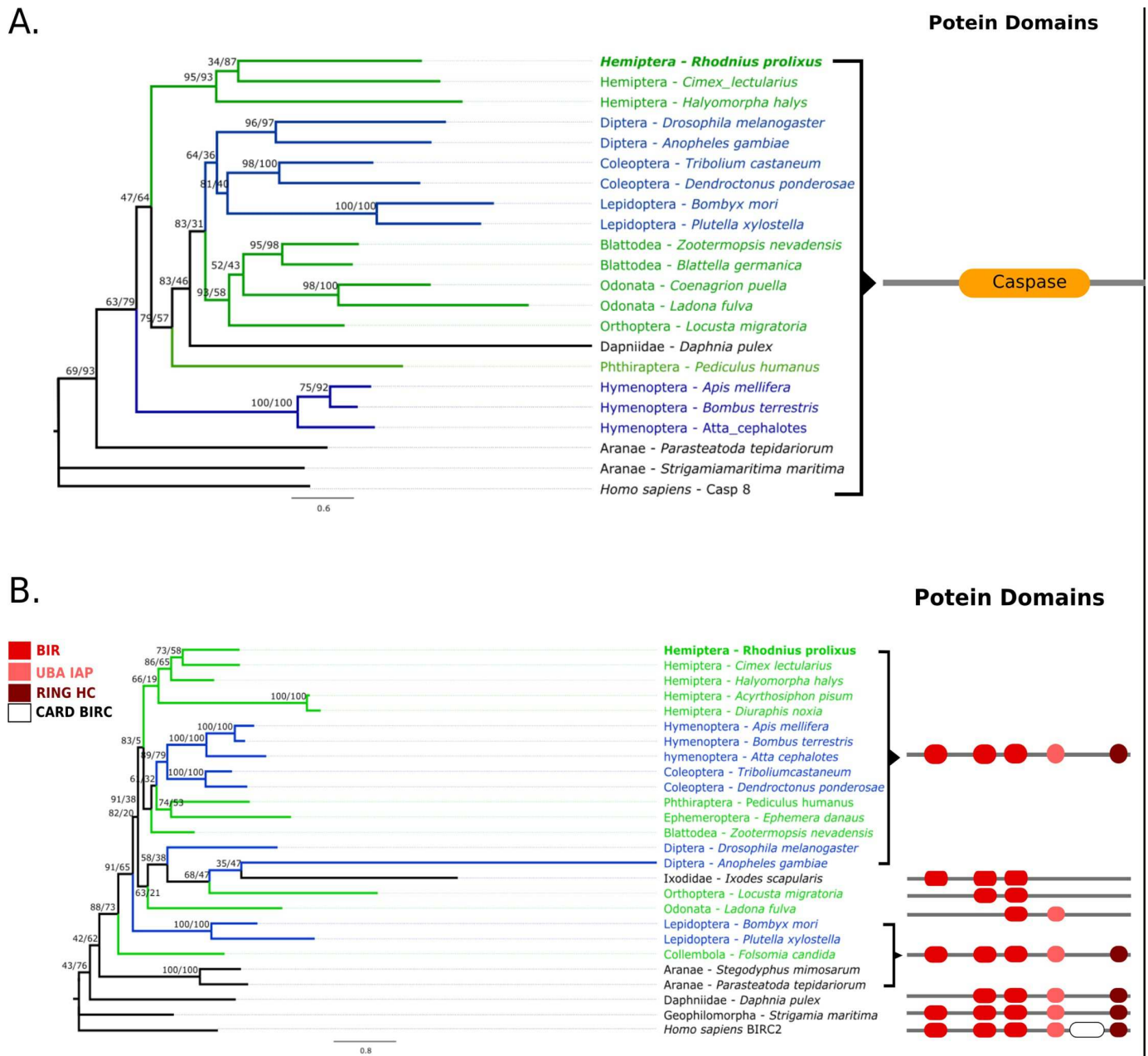


Fig 2. DREDD and CASPAR Maximum likelihood phylogenetic trees in selected arthropods. (A) rpDREDD forms a clade with other hemipterans but is distinct from other hemimetabolous insects (green). (B) rpCASPAR forms a clade with other paraneopteran insects except for aphids which form a distinct clade basal to most insects. The human Caspase 8 and FAF1 were used as outgroups to build the ML trees.

<https://doi.org/10.1371/journal.pone.0214794.g002>

be either rpEffete, rpUev1a, or rpBendless orthologs. The resulting BLAST hits for the three searches were very similar for different metrics (e.g. low e-values and high identity). Therefore, a ML tree was built with orthologs of these 3 genes to elucidate their identity (Fig 4). The topology of this tree confirms the HMM-profile searches results, separating the 3 orthologs into different clades (RPRC005317 within rpEffete clade, RPRC011375 within rpUev1a clade, and RPRC011790 within rpBendless clade). Effete and Bendless orthologs are in single clades but

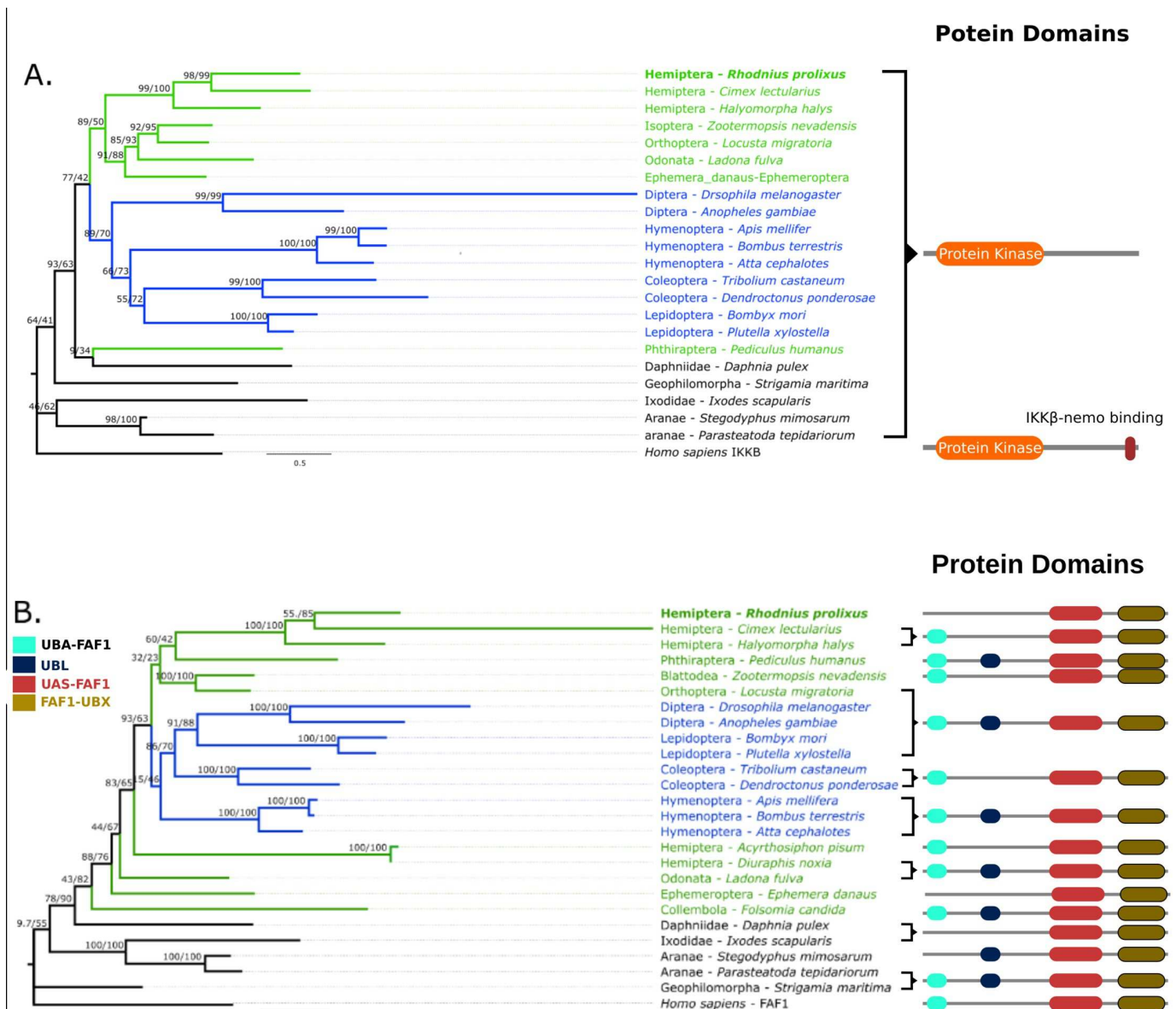


Fig 3. IKKβ and IAP2 Maximum likelihood phylogenetic trees in selected arthropods. (A) rplIKKβ forms a clade with other hemimetabolous insects (except *P. humanus*) and is a sister clade to all other insects, but different from other arthropod groups. (B) rplIAP2 forms a clade with other hemipterans and is a sister clade to all hymenopterans and coleopterans insects. The human IKKβ ortholog was used as an outgroup to build the ML trees.

<https://doi.org/10.1371/journal.pone.0214794.g003>

the internal branches are poorly supported, likely due to the high protein sequence similarity among these three molecules (Identity percentage > 98%).

Ubiquitin carboxyl-terminal hydrolase Cyindrmatosis (CYLD)

The Cyindrmatosis CYLD ortholog in *R. prolixus* (rpCYLD) has a similar domain architecture to the *Drosophila* CYLD, with 2 CAP-Gly domains and 1 Peptidase-C19 domain. The ML-tree shows rpCYLD in a clade with other hemipterans, sister to all holometabolous insect CYLD orthologs (Fig 5).

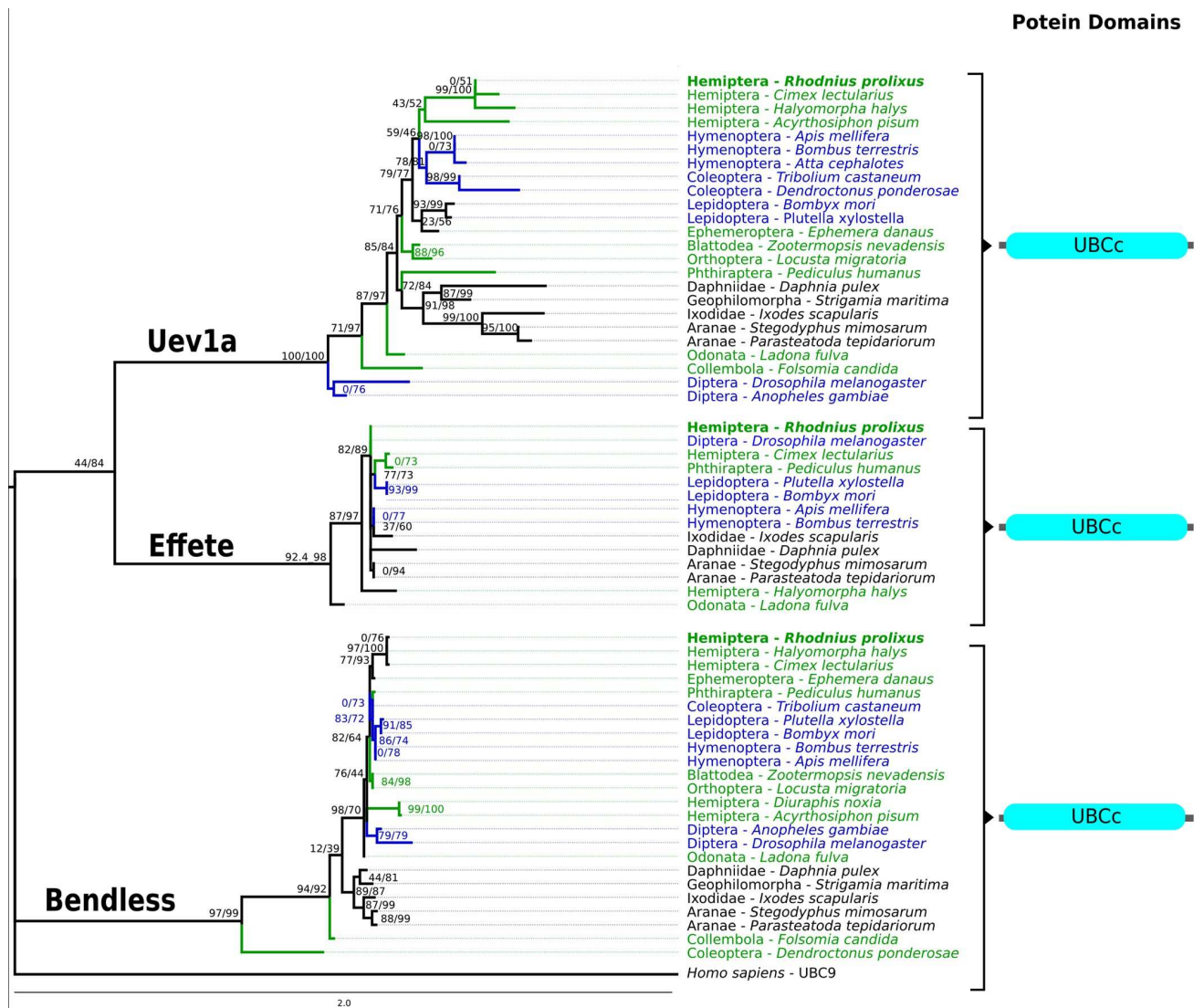


Fig 4. Uev1a, Effete, and Bendless Maximum likelihood phylogenetic trees in selected arthropods. These ubiquitin conjugating enzymes share an UBCc domain that constitutes most of their structure. Orthologs of each of these proteins are contained in a single clade separate from the other protein clades. The human UBC9 was used as outgroup to build the ML trees.

<https://doi.org/10.1371/journal.pone.0214794.g004>

Differential AMP expression in the fat body

The expression of AMPs in the fat body of *R. prolixus* was compared 8h after intrathoracic injection of Gram-negative or Gram-positive bacteria. Transcript levels for each AMP were compared with the levels expressed in PBS injected insects serving as the second calibrator ($\Delta\Delta CT$ [57,58]). The expression of all AMPs was similar after injection with Gram-positive or Gram-negative bacteria (Fig 6A). Only Defensin-C showed a significant induction after injection with Gram-negative bacteria (CI_{95} 1.01–3.16) and a suppression after injection of Gram-positive bacteria (CI_{95} 0.06–0.19). rpRelish levels were lower in insects injected with Gram-positive bacteria compared with insects injected with PBS (CI_{95} –0.12–0.62)

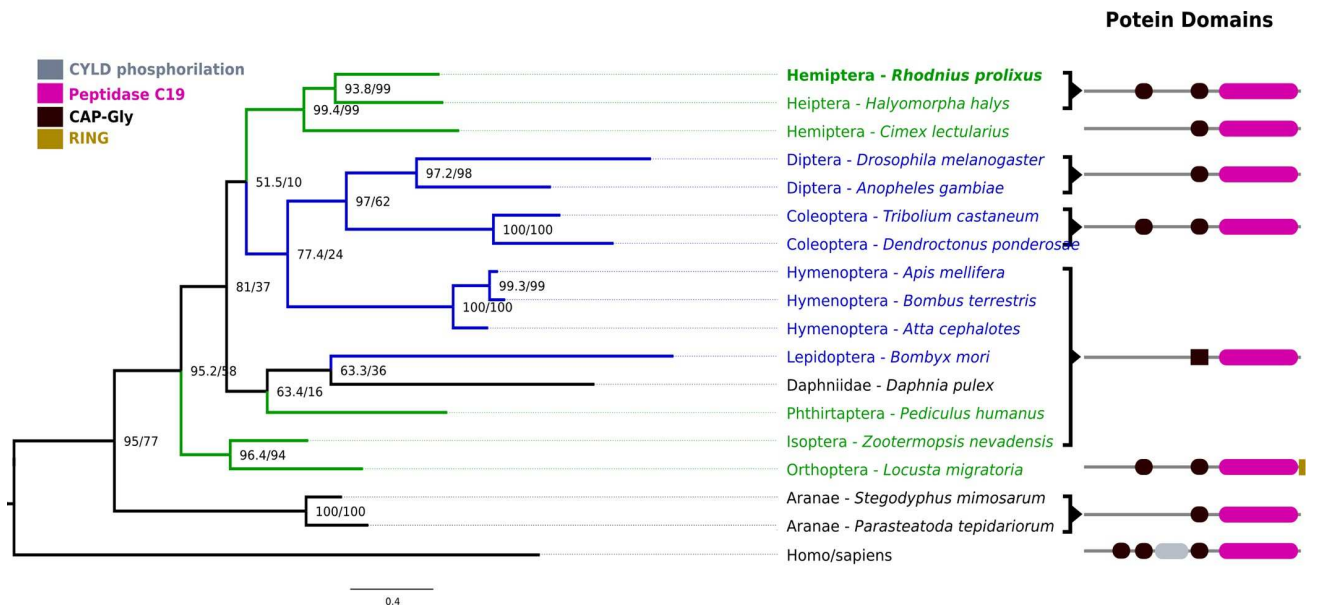


Fig 5. CYLD Maximum likelihood phylogenetic tree in selected arthropods. Hemimetabolous insects are divided among three clades, comprising hemipterans, phthirapterans, and paraneopterans. Most holometabolous insects form a clade that clusters with the hemipteran clade including rpCYLD. The human UBC9 was used as outgroup to build the ML trees.

<https://doi.org/10.1371/journal.pone.0214794.g005>

The effect of silencing rpRelish on AMP transcription

AMP transcript levels were measured 8h after intrathoracic inoculation of bacteria into insects that had received dsRNA. In these experiments, AMP expression levels were compared between insects that had been injected with dsANT or dsRelish. rpRelish knockdown reduced rpRelish expression by 88% compared with dsANT injected insects that later were injected with Gram-negative bacteria, and by 94% compared with dsANT injected that later were injected with Gram-positive bacteria (Fig 6B and 6C).

In rpRelish silenced insects injected with Gram-negative bacteria, Prolixicin, Lysozyme-B, and Defensin-A expression decreased to 47% (CI₉₅ 24% - 70%), 48% (CI₉₅ 11% - 84%) and 46% (CI₉₅ 28% - 66%) respectively of their dsANT injected controls. Defensin-C transcripts levels showed a high degree of variation, with no evidence of differential transcription between dsANT and dsRelish treated insects (Fig 6B). After infection with Gram-positive bacteria, only Prolixicin showed significant changes in expression with transcript levels reduced to 55% (CI₉₅ 31%-80%) of dsANT injected insects (Fig 6C).

Discussion

Homolog search

Using a combination of reciprocal BLAST searches and the construction of taxonomically unbiased HMMs we found novel orthologs that represent most of the “missing” members of the IMD pathway in *R. prolixus*. Hidden Markov model searches outperformed reciprocal BLAST searches, but both strategies found the same candidate genes if they were annotated in the genome. Zumaya-Estrada et al [59] used similar homology search strategies and found several IMD pathway genes [59], while Ribeiro et al found a Caspar homolog in a midgut transcriptome [40]. In our analysis of published transcriptomes, we found 3 additional genes that are not currently annotated in the *R. prolixus* genome. We were unable, however, to find

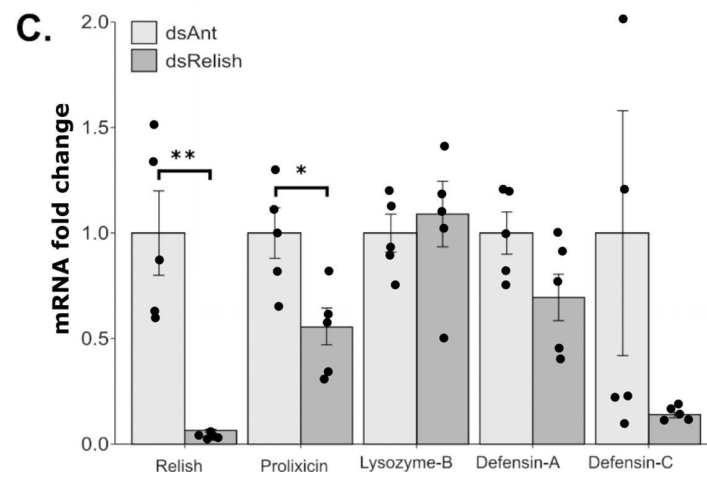
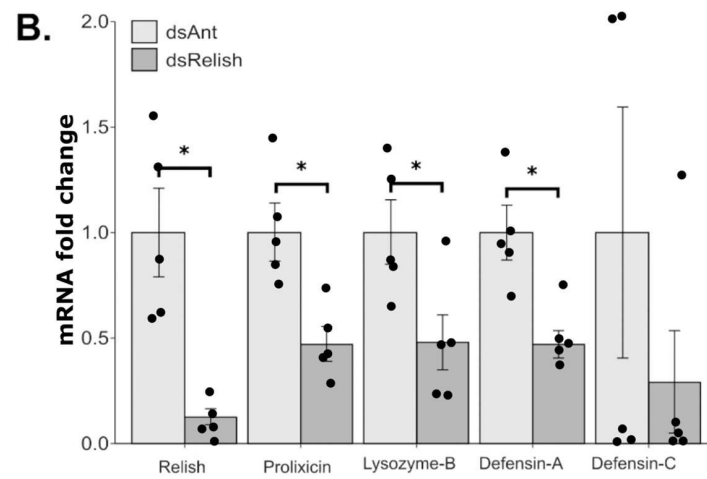
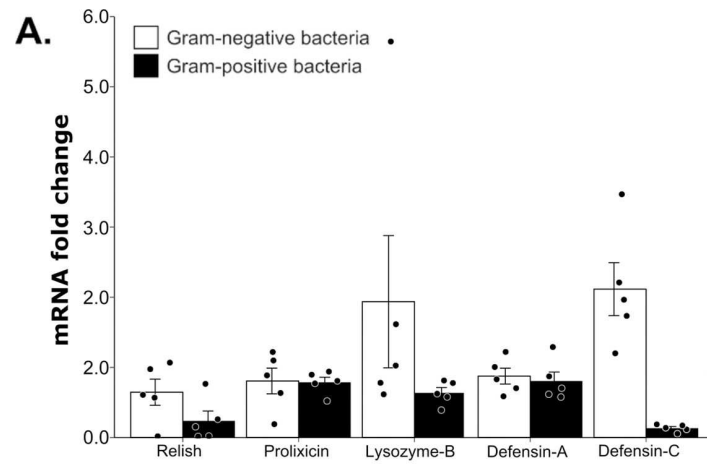


Fig 6. Fat body AMP expression in 5th instar *Rhodnius prolixus* infected with Gram-negative and Gram-positive bacteria. (A) Relative AMP expression in nymphs injected with *Enterobacter doacae* (Gram-negative) and *Staphylococcus aureus* (Gram-positive) bacteria. Relative expression levels in each gene used levels in the PBS injected insects as the second calibrator, which is assigned a value of 1 in all comparisons as described in [57]. The effect of silencing rpRelish was assessed in insects injected with (B) *Enterobacter doacae* (Gram-negative bacteria) or (C) *Staphylococcus aureus* (Gram-positive bacteria). Insects were injected with 2.5 μ g of dsRNA complementary to Relish mRNA or ANT, a plant gene that serves as a dsRNA injection control. Four days later insects were injected intrathoracically with 10⁸ bacteria. AMP transcripts were measured 8h after injection with bacteria. Expression analysis used the $\Delta\Delta$ CT method [57] and data are presented as fold differences between dsRelish and dsANT silenced insects. Bars represent the mean transcript levels \pm SEM in 5 replicates of 3 pooled fat bodies. Means were compared using the unpaired Student's T-test. [†]P < 0.05, ^{**}P < 0.01. Treatments that did not follow a normal distribution (Lys-B in Gram-negative bacteria injection and Def-C in dsANT injection) based on the Shapiro-Wilk normality test (p-values > 0.05, S1 Table), were compared with the Mann Whitney U Test.

<https://doi.org/10.1371/journal.pone.0214794.g006>

orthologs for IMD and Kenny. These data suggest that the annotated genelist from *R. prolixus* is incomplete. Software regularly used to annotate genomes uses ab-initio approaches based on the structure of known genes. Hemipterans seem to have an unusual gene structure with genes made of shorter exons than other insects [60]. Consequently, ab-initio approaches based on non-hemipteran insects might not provide accurate gene models. Gene prediction software such as Augustus and MAKER can be trained to generate relevant gene models for hemipterans as they allow approaches to combine data from transcriptomes, EST, and genomes from taxonomically closer organisms [61,62]. Therefore, the assumed absence of IMD pathway genes in many arthropods could be explained either by the absence of orthologs or by the difficulty in finding these genes. In this study, we adapted a strategy from Palmer and Jiggins [12] that combines genomic and transcriptomic data and the use of HMM to better predict distant homologs. It is important to recall, however, that genomic and transcriptomic data are not infallible and that even accurate gene models can fail to predict genes. In the milk weed bug genome project, for example, an IMD gene was only found by classic cloning and the use of degenerate primers after the failure of genomic and transcriptomic sequencing to identify strong candidate molecules.

Evolution of IMD pathway genes

The IMD pathway is the most variable immune pathway in arthropods [12,63], and hemipterans are the principal insect group with a reported gene reduction [13,37,59,60,64–67]. After a closer inspection of the IMD pathway in hemipterans, we found that insects in the Sternorrhyncha superfamily (Planthoppers, whiteflies, and aphids) indeed have a loss of important membrane-proximal signaling genes (PGRP, IMD, FADD, and DREDD, and Relish) and the NF- κ B transcription factor Relish (Fig 7). The absence of these genes could be an adaptation in sternorrhynchans related to the specialized feeding habits and highly specific relationships they have with symbiotic bacteria that provide essential amino acids and nutrients [68,69]. Sternorrhynchans, in general, are missing multiple elements of the IMD pathway, including *D. citrii*, which is considered in most phylogenetic trees to be basal to the other members of this group, and *A. pisium*, considered to be more derived. On the other hand, we found a very complete pathway for most heteropteran insects (true bugs) and the large milk weed bug, *Oncopeltus fasciatus*, seems to have a complete IMD pathway with orthologs for IMD, FADD, and DREDD. All other heteropterans lack at least one of these genes, and all but the brown planthopper, *Nilaparvata lugens*, are lacking orthologs for Kenny. The absence of IMD itself is especially intriguing since this molecule is central to the operation of the pathway. In *Drosophila*, IMD interacts with PGRPs and FADD; it is cleaved by DREDD, and K63-ubiquitinated by IAP2 [4]. An alternative activation of the IMD pathway may exist in *R. prolixus*. One possibility is that FADD can transduce the IMD pathway signaling in the absence of IMD. Another

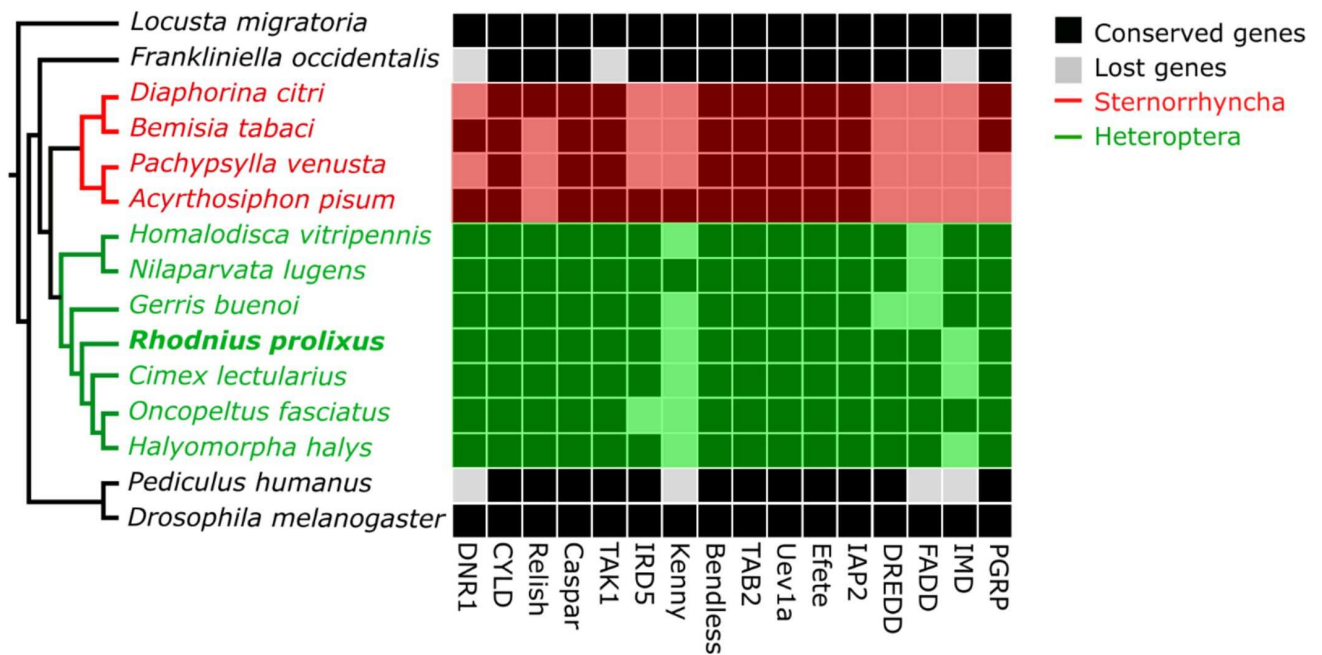


Fig 7. IMD pathway gene orthologs in selected insects. The presence of gene orthologs in several selected holo- and hemimetabolous insects is compared with their phylogeny. Orthologs that are present are shown as black boxes and absent orthologs are shown as white boxes. The tree indicates heteropterans, including *Rhodnius prolixus* in green, the sternorrhyncha, including aphids, whiteflies, and scale insects, are in red and holometabolous insects and paraneopterans are in black. The phylogenetic relationships among the species shown were modified after [70].

<https://doi.org/10.1371/journal.pone.0214794.g007>

alternative is the existence of a novel protein that functions as IMD, or the cryptic functioning of another protein acting as IMD. While our methodology to find distant orthologs is very sensitive, we cannot discard the possibility that the absence of IMD is due to further sequence divergence of this gene. The use of biochemical assays will help elucidate these scenarios.

The IMD pathway evolved early in arthropods and orthologs for this pathway are found in crustaceans, polyneopterans, and holometabolous insects. It has been proposed, across a broad range of taxa, that immune related genes are among the most rapidly evolving genes [71,72]. IMD pathway genes show significantly more sequence divergence among insect species than genes in other immune pathways, which might suggest that hemipterans faced different selective pressures in the evolution of this pathway [4,10,12,73]. Indeed, the IMD pathway has stronger positive selection than other pathways in *Drosophila* [74–76] and termites [77]. Genes with evidence of positive selection in these insects are involved in signal transduction (e.g. Relish, Dredd, IKK-β, and DNR1) and it has been hypothesized that pathogens are driving the adaptive evolution of these molecules [77,78]. Hemipterans have a strong association with endosymbionts [79–81] that could trigger higher rates of evolution throughout the whole pathway, but this needs to be addressed formally. One explanation of why the IMD pathway is more variable than other immune pathways and might be more adaptable to symbiotic and pathogenic responses, is that it is not closely linked to developmental processes as is the case of the Toll pathway.

Many of the organisms that have a modified IMD pathway also have specialized diets such as sap feeding in aphids or obligate hematophagy in bedbugs and kissing bugs. It has been proposed that such specialized diets contribute to the evolution of a reduced immune system because i) these diets contain few microorganisms and therefore do not require a robust immune activation, and ii) symbiotic organisms are tolerated by reduced immune systems

because they provide nutrients that are absent in the limited diet [82]. Our findings do not fully support these hypotheses in *R. prolixus*. Our updated IMD pathway in *R. prolixus* resembles those from non-hematophagous insects and is activated during bacterial infections. Furthermore, kissing bugs are gregarious insects that live in non-sterile environments. Feeding is not restricted to sterile blood; early instar nymphs acquire obligate symbionts through coprophagy and hemolymphagy and phytophagy occur in triatomines, challenging the convention that they are strictly hematophagous [83–85]. The evolution of tolerance mechanisms towards bacterial symbionts exist in other insects and do not involve the depletion of immune related genes. Intracellular bacteria in tsetse flies are found in a bacteriosome that downregulates the IMD pathway by producing PGRP-LB [86]. This PGN amidase degrades the PAMP that activates the pathway, therefore protecting the endosymbiont. This mechanism also operates in the weevil *Strophilus zeamais* [87]. The principal endosymbiont of *R. prolixus*, *Rhodococcus rhodnii*, provides B-complex vitamins, similar to the role played by *Wigglesworthia* sp in tsetse flies. *Rhodococcus* sp., however, is extracellular, does not form bacteriosomes, and therefore would require different tolerance mechanisms. It is likely that such tolerance mechanisms would be mediated by the IMD and Toll pathways since silencing of dorsal (Toll pathway transcription factor) increases the bacterial population in the midgut while silencing of Relish induces a reduction in bacterial populations [37].

IMD pathway control of AMPs

AMPs are regulated directly by the Toll and IMD pathways in arthropods. In *Drosophila*, the Toll pathway is reported to respond to infections with fungi and Gram-positive bacteria while the IMD pathway is activated by Gram-negative bacteria, and each pathway induces the expression of a subset of AMPs. Recent studies, however, indicate that AMP expression can be coregulated by the IMD, Toll, and JAK-STAT pathways [88–90]. In *R. prolixus*, we demonstrated that the IMD pathway principally regulates AMP expression against Gram-negative bacteria (Fig 6A and 6B) compared with infections with Gram-positive bacteria (Fig 6A and 6C). The expression of all the AMPs we measured was reduced in insects in which rpRelish expression was reduced using RNAi and posteriorly injected with Gram-negative bacteria, suggesting that the IMD pathway is regulating the levels of all AMPs. Interestingly silencing of rpRelish also regulates AMP expression after infection with Gram-positive bacteria. These results differ from the *Drosophila* model and suggest an interaction between recognition or signaling events of the IMD and Toll pathways. Nishide et al reported a strong crosstalk between these pathways in the heteropteran *Plautia stali* [9]. In their model, insects injected with Gram-positive or Gram-negative bacteria upregulated the same AMPs. Furthermore, silencing the Toll or IMD pathways reduced a subset of these AMPs. Maximum suppression of all AMP expression was achieved by co-silencing both pathways. This study and ours using RNAi support the hypothesis of a coregulation of AMP expression by both pathways, but also indicate that one pathway predominately regulates each AMP. Although we did not measure the influence of the Toll pathway in *R. prolixus*, the expression patterns of Prolixicin and Defensin-C suggests they are likely regulated by the Toll pathway.

This coregulation concept is not limited to hemimetabolous insects. The expression of Gambicin in *Aedes aegypti* is regulated by transcription factors of the IMD and JAK-STAT pathways [88]. This might be the case with Defensin-C in *R. prolixus* as there is a STAT binding site 174bp upstream of the coding region. Defensin-A and Lysozyme-B, however, have a NF- κ B binding site at this same location that could make the regulation of these genes more responsive to Relish or Dorsal than STAT [33]. Surprisingly, Prolixicin expression is dependent on Relish despite not having an obvious NF- κ B binding domains in its promoter region

[32] but the discordant expression of AMPs in the fat body and in different sections of the midgut cannot be explained solely by IMD NF- κ B sites. STAT and Toll NF- κ B binding sites may provide additional regulation that accounts for these differences. A systematic analysis of AMP promoters might help determine factors in the co-regulation of AMPs by multiple regulatory pathways.

Regardless of the combination of factors that contribute to the expression and regulation of multiple AMPs, we have identified molecules that fill in many of the reported gaps in the *R. prolixus* IMD pathway. In contrast to the conclusions of the *R. prolixus* genome paper [36], our data indicate that this pathway is functional and inducible in *R. prolixus* and now can be considered very similar to the described IMD pathways of holometabolous insects.

Supporting information

S1 File. Amino acid sequence alignments used to generate the phylogenetic trees and the HMM profiles. Accession numbers are reported alongside the sequences.
(TXT)

S1 Supporting Data. mRNA fold change data for AMPs used to build Fig 6.
(XLSX)

S1 Table. *Rhodnius prolixus* IMD pathway homologs with genes reported in GenBank and Vector Base amplified with the described primers using *Rhodnius prolixus* fat body cDNA. The resulting sequences are available in GenBank under accession numbers beginning with MH.
(DOCX)

S2 Table. Primers for the generation of dsRNA for use in silencing assays. Each gene was first PCR amplified with primers in bold. These PCR amplicons then were used as template for a second PCR with primers that included the 5' T7 promoter (complete sequence). PCR amplification profiles and purification procedures are described in the Methods section.
(DOCX)

S3 Table. Primers for quantitative real time PCR. Primers were designed using the PRIMER3, Beacon Designer™, and mFOLD.
(DOCX)

Acknowledgments

We thank Luciana de Lima Ferreira, Newmar Pinto Marliere, Maria Raquel Araujo dos Santos, Felipe de Almeida Dias, Ana Caroline Paiva, Octávio A. Talyuli, Tainan Carla Guedes and Heather Coatsworth for training and technical support. We thank Sydne Guevara Rozo and Heather Coatsworth for critical reading and comments.

Author Contributions

Conceptualization: Nicolas Salcedo-Porras, Pedro L. Oliveira, Carl Lowenberger.

Formal analysis: Nicolas Salcedo-Porras, Alessandra Guarneri, Pedro L. Oliveira, Carl Lowenberger.

Funding acquisition: Carl Lowenberger.

Investigation: Nicolas Salcedo-Porras, Alessandra Guarneri, Pedro L. Oliveira, Carl Lowenberger.

Methodology: Nicolas Salcedo-Porras, Alessandra Guarneri, Pedro L. Oliveira, Carl Lowenberger.

Project administration: Carl Lowenberger.

Resources: Carl Lowenberger.

Supervision: Alessandra Guarneri, Pedro L. Oliveira, Carl Lowenberger.

Validation: Nicolas Salcedo-Porras.

Writing – original draft: Nicolas Salcedo-Porras.

Writing – review & editing: Alessandra Guarneri, Pedro L. Oliveira, Carl Lowenberger.

References

1. Kimbrell DA, Beutler B. The evolution and genetics of innate immunity. *Nat Rev Genet.* 2001; 2: 256–267. <https://doi.org/10.1038/35066006> PMID: [11283698](https://pubmed.ncbi.nlm.nih.gov/11283698/)
2. Valanne S, Wang J-H, Rämét M. The *Drosophila* Toll signaling pathway. *J Immunol.* 2011; 186: 649–656. <https://doi.org/10.4049/jimmunol.1002302> PMID: [21209287](https://pubmed.ncbi.nlm.nih.gov/21209287/)
3. Myllymäki H, Valanne S, Rämét M. The *Drosophila* Imd signaling pathway. *J Immunol.* 2014; 192: 3455–3462. <https://doi.org/10.4049/jimmunol.1303309> PMID: [24706930](https://pubmed.ncbi.nlm.nih.gov/24706930/)
4. Kleino A, Silverman N. The *Drosophila* IMD pathway in the activation of the humoral immune response. *Dev Comp Immunol.* 2014; 42: 25–35. <https://doi.org/10.1016/j.dci.2013.05.014> PMID: [23721820](https://pubmed.ncbi.nlm.nih.gov/23721820/)
5. Morin-Poulard I, Vincent A, Crozatier M. The *Drosophila* JAK-STAT pathway in blood cell formation and immunity. *JAKSTAT.* 2013; 2: e25700. <https://doi.org/10.4161/jkst.25700> PMID: [24069567](https://pubmed.ncbi.nlm.nih.gov/24069567/)
6. Lindsay SA, Wasserman SA. Conventional and non-conventional *Drosophila* Toll signaling. *Dev Comp Immunol.* 2014; 42: 16–24. <https://doi.org/10.1016/j.dci.2013.04.011> PMID: [23632253](https://pubmed.ncbi.nlm.nih.gov/23632253/)
7. Ganesan S, Aggarwal K, Paquette N, Silverman N. NF- κ B/Rel proteins and the humoral immune responses of *Drosophila melanogaster*. *Curr Top Microbiol Immunol.* 2011; 349: 25–60. https://doi.org/10.1007/82_2010_107 PMID: [20852987](https://pubmed.ncbi.nlm.nih.gov/20852987/)
8. Tanji T, Hu X, Weber ANR, Ip YT. Toll and IMD pathways synergistically activate an innate immune response in *Drosophila melanogaster*. *Mol Cell Biol.* 2007; 27: 4578–4588. <https://doi.org/10.1128/MCB.01814-06> PMID: [17438142](https://pubmed.ncbi.nlm.nih.gov/17438142/)
9. Nishide Y, Kageyama D, Yokoi K, Jouraku A, Tanaka H, Futahashi R, et al. Functional crosstalk across IMD and Toll pathways: insight into the evolution of incomplete immune cascades. *Proceedings of the Royal Society B: Biological Sciences.* 2019; 286: 20182207. <https://doi.org/10.1098/rspb.2018.2207>
10. Lai AG, Aboobaker AA. Comparative genomic analysis of innate immunity reveals novel and conserved components in crustacean food crop species. *BMC Genomics.* 2017; 18: 389. <https://doi.org/10.1186/s12864-017-3769-4> PMID: [28521727](https://pubmed.ncbi.nlm.nih.gov/28521727/)
11. Shaw DK, Wang X, Brown LJ, Chávez ASO, Reif KE, Smith AA, et al. Infection-derived lipids elicit an immune deficiency circuit in arthropods. *Nat Commun.* 2017; 8: 14401. <https://doi.org/10.1038/ncomms14401> PMID: [28195158](https://pubmed.ncbi.nlm.nih.gov/28195158/)
12. Palmer WJ, Jiggins FM. Comparative genomics reveals the origins and diversity of arthropod immune systems. *Mol Biol Evol.* 2015; 32: 2111–2129. <https://doi.org/10.1093/molbev/msv093> PMID: [25908671](https://pubmed.ncbi.nlm.nih.gov/25908671/)
13. Elsik CG. The pea aphid genome sequence brings theories of insect defense into question. *Genome Biol.* 2010; 11: 106. <https://doi.org/10.1186/gb-2010-11-2-106> PMID: [20236492](https://pubmed.ncbi.nlm.nih.gov/20236492/)
14. Kim JH, Min JS, Kang JS, Kwon DH, Yoon KS, Strycharz J, et al. Comparison of the humoral and cellular immune responses between body and head lice following bacterial challenge. *Insect Biochem Mol Biol.* 2011; 41: 332–339. <https://doi.org/10.1016/j.ibmb.2011.01.011> PMID: [21296152](https://pubmed.ncbi.nlm.nih.gov/21296152/)
15. Armitage SAO, Peuss R, Kurtz J. Dscam and pancrustacean immune memory—a review of the evidence. *Dev Comp Immunol.* 2015; 48: 315–323. <https://doi.org/10.1016/j.dci.2014.03.004> PMID: [24657209](https://pubmed.ncbi.nlm.nih.gov/24657209/)
16. Chagas C. Nova tripanozomíase humana: estudos sobre a morfologia e o ciclo evolutivo do *Schizotrypanum cruzi* n. gen., n. sp., agente etiológico de nova entidade morbida do homem. *Mem Inst Oswaldo Cruz.* 1909; 1: 159–218. <https://doi.org/10.1590/S0074-02761909000200008>
17. Snodgrass RE. The principles of insect physiology. *Science.* 1939; 90: 159–159. <https://doi.org/10.1126/science.90.2329.159-a> PMID: [17829328](https://pubmed.ncbi.nlm.nih.gov/17829328/)

18. TEJERA Gr. E. La Trypanosome americana ou maladie de Chagas au Venezuela. Bulletin de la Société de Pathologie Exotique. 1919; 12: 509–513. Available: <https://www.cabdirect.org/cabdirect/abstract/19202900678>
19. Chagas disease in Latin America: an epidemiological update based on 2010 estimates. Wkly Epidemiol Rec. 2015; 90: 33–43. PMID: [25671846](https://pubmed.ncbi.nlm.nih.gov/25671846/)
20. World Health Organization, Savioli L, Daumerie D, World Health Organization Department of Control of Neglected Tropical Diseases. Sustaining the drive to overcome the global impact of neglected tropical diseases: Second WHO report on neglected tropical diseases. Geneva, Switzerland: World Health Organization;
21. Mello CB, Garcia ES, Ratcliffe NA, Azambuja P. Trypanosoma cruzi and Trypanosoma rangeli: interplay with hemolymph components of *Rhodnius prolixus*. J Invertebr Pathol. 1995; 65: 261–268. <https://doi.org/10.1006/jipa.1995.1040> PMID: [7745280](https://pubmed.ncbi.nlm.nih.gov/7745280/)
22. Whitten MM, Mello CB, Gomes SA, Nigam Y, Azambuja P, Garcia ES, et al. Role of superoxide and reactive nitrogen intermediates in *Rhodnius prolixus* (Reduviidae)/*Trypanosoma rangeli* interactions. Exp Parasitol. 2001; 98: 44–57. <https://doi.org/10.1006/expr.2001.4615> PMID: [11426951](https://pubmed.ncbi.nlm.nih.gov/11426951/)
23. Azambuja P, Feder D, Garcia ES. Isolation of *Serratia marcescens* in the midgut of *Rhodnius prolixus*: impact on the establishment of the parasite *Trypanosoma cruzi* in the vector. Exp Parasitol. 2004; 107: 89–96. <https://doi.org/10.1016/j.exppara.2004.04.007> PMID: [15208042](https://pubmed.ncbi.nlm.nih.gov/15208042/)
24. Castro DP, Moraes CS, Gonzalez MS, Ratcliffe NA, Azambuja P, Garcia ES. Trypanosoma cruzi immune response modulation decreases microbiota in *Rhodnius prolixus* gut and is crucial for parasite survival and development. PLoS One. 2012; 7: e36591. <https://doi.org/10.1371/journal.pone.0036591> PMID: [22574189](https://pubmed.ncbi.nlm.nih.gov/22574189/)
25. Ferreira RC, Kessler RL, Lorenzo MG, Paim RMM, Ferreira LDL, Probst CM, et al. Colonization of *Rhodnius prolixus* gut by *Trypanosoma cruzi* involves an extensive parasite killing. Parasitology. 2016; 143: 434–443. <https://doi.org/10.1017/S0031182015001857> PMID: [26818093](https://pubmed.ncbi.nlm.nih.gov/26818093/)
26. Dias F de A, Guerra B, Vieira LR, Perdomo HD, Gandara ACP, Amaral RJV do, et al. Monitoring of the Parasite Load in the Digestive Tract of *Rhodnius prolixus* by Combined qPCR Analysis and Imaging Techniques Provides New Insights into the Trypanosome Life Cycle. PLoS Negl Trop Dis. 2015; 9: e0004186. <https://doi.org/10.1371/journal.pntd.0004186> PMID: [26496442](https://pubmed.ncbi.nlm.nih.gov/26496442/)
27. Garcia ES, Genta FA, de Azambuja P, Schaub GA. Interactions between intestinal compounds of triatomines and *Trypanosoma cruzi*. Trends Parasitol. 2010; 26: 499–505. <https://doi.org/10.1016/j.pt.2010.07.003> PMID: [20801082](https://pubmed.ncbi.nlm.nih.gov/20801082/)
28. Flores-Villegas AL, Salazar-Schettino PM, Córdoba-Aguilar A, Gutiérrez-Cabrera AE, Rojas-Wastavino GE, Bucio-Torres MI, et al. Immune defence mechanisms of triatomines against bacteria, viruses, fungi and parasites. Bull Entomol Res. 2015; 105: 523–532. <https://doi.org/10.1017/S0007485315000504> PMID: [26082354](https://pubmed.ncbi.nlm.nih.gov/26082354/)
29. Guarneri AA, Lorenzo MG. Triatomine physiology in the context of trypanosome infection. J Insect Physiol. 2017; 97: 66–76. <https://doi.org/10.1016/j.jinsphys.2016.07.005> PMID: [27401496](https://pubmed.ncbi.nlm.nih.gov/27401496/)
30. Vieira CS, Mattos DP, Waniek PJ, Santangelo JM, Figueiredo MB, Gumiel M, et al. *Rhodnius prolixus* interaction with *Trypanosoma rangeli*: modulation of the immune system and microbiota population. Parasit Vectors. 2015; 8: 135. <https://doi.org/10.1186/s13071-015-0736-2> PMID: [25888720](https://pubmed.ncbi.nlm.nih.gov/25888720/)
31. Vieira CS, Waniek PJ, Castro DP, Mattos DP, Moreira OC, Azambuja P. Impact of *Trypanosoma cruzi* on antimicrobial peptide gene expression and activity in the fat body and midgut of *Rhodnius prolixus*. Parasit Vectors. 2016; 9: 119. <https://doi.org/10.1186/s13071-016-1398-4> PMID: [26931761](https://pubmed.ncbi.nlm.nih.gov/26931761/)
32. Ursic-Bedoya R, Buchhop J, Joy JB, Durvasula R, Lowenberger C. Prolixicin: a novel antimicrobial peptide isolated from *Rhodnius prolixus* with differential activity against bacteria and *Trypanosoma cruzi*. Insect Mol Biol. 2011; 20: 775–786. <https://doi.org/10.1111/j.1365-2583.2011.01107.x> PMID: [21906194](https://pubmed.ncbi.nlm.nih.gov/21906194/)
33. Ursic-Bedoya RJ, Nazzari H, Cooper D, Triana O, Wolff M, Lowenberger C. Identification and characterization of two novel lysozymes from *Rhodnius prolixus*, a vector of Chagas disease. J Insect Physiol. 2008; 54: 593–603. <https://doi.org/10.1016/j.jinsphys.2007.12.009> PMID: [18258253](https://pubmed.ncbi.nlm.nih.gov/18258253/)
34. Vieira CS, Waniek PJ, Mattos DP, Castro DP, Mello CB, Ratcliffe NA, et al. Humoral responses in *Rhodnius prolixus*: bacterial feeding induces differential patterns of antibacterial activity and enhances mRNA levels of antimicrobial peptides in the midgut. Parasit Vectors. 2014; 7: 232. <https://doi.org/10.1186/1756-3305-7-232> PMID: [24885969](https://pubmed.ncbi.nlm.nih.gov/24885969/)
35. Lopez L, Morales G, Ursic R, Wolff M, Lowenberger C. Isolation and characterization of a novel insect defensin from *Rhodnius prolixus*, a vector of Chagas disease. Insect Biochem Mol Biol. 2003; 33: 439–447. [https://doi.org/10.1016/S0965-1748\(03\)00008-0](https://doi.org/10.1016/S0965-1748(03)00008-0) PMID: [12650692](https://pubmed.ncbi.nlm.nih.gov/12650692/)

36. Ursic-Bedoya RJ, Lowenberger CA. *Rhodnius prolixus*: identification of immune-related genes up-regulated in response to pathogens and parasites using suppressive subtractive hybridization. *Dev Comp Immunol*. 2007; 31: 109–120. <https://doi.org/10.1016/j.dci.2006.05.008> PMID: 16824597
37. Mesquita RD, Vionette-Amaral RJ, Lowenberger C, Rivera-Pomar R, Monteiro FA, Minx P, et al. Genome of *Rhodnius prolixus*, an insect vector of Chagas disease, reveals unique adaptations to hematophagy and parasite infection. *Proc Natl Acad Sci USA*. 2015; 112: 14936–14941. <https://doi.org/10.1073/pnas.1506226112> PMID: 26627243
38. Benoit JB, Adelman ZN, Reinhardt K, Dolan A, Poelchau M, Jennings EC, et al. Unique features of a global human ectoparasite identified through sequencing of the bed bug genome. *Nat Commun*. 2016; 7: 10165. <https://doi.org/10.1038/ncomms10165> PMID: 26836814
39. Kirkness EF, Haas BJ, Sun W, Braig HR, Perotti MA, Clark JM, et al. Genome sequences of the human body louse and its primary endosymbiont provide insights into the permanent parasitic lifestyle. *Proc Natl Acad Sci USA*. 2010; 107: 12168–12173. <https://doi.org/10.1073/pnas.1003379107> PMID: 20566863
40. Ribeiro JMC, Genta FA, Sorgine MHF, Logullo R, Mesquita RD, Paiva-Silva GO, et al. An insight into the transcriptome of the digestive tract of the bloodsucking bug, *Rhodnius prolixus*. *PLoS Negl Trop Dis*. 2014; 8: e2594. <https://doi.org/10.1371/journal.pntd.0002594> PMID: 24416461
41. Bao Y-Y, Qu L-Y, Zhao D, Chen L-B, Jin H-Y, Xu L-M, et al. The genome- and transcriptome-wide analysis of innate immunity in the brown planthopper, *Nilaparvata lugens*. *BMC Genomics*. 2013; 14: 160. <https://doi.org/10.1186/1471-2164-14-160> PMID: 23497397
42. Gramates LS, Marygold SJ, Santos GD, Urbano J-M, Antonazzo G, Matthews BB, et al. FlyBase at 25: looking to the future. *Nucleic Acids Res*. 2017; 45: D663–D671. <https://doi.org/10.1093/nar/gkw1016> PMID: 27799470
43. Brucker RM, Funkhouser LJ, Setia S, Pauly R, Bordenstein SR. Insect Innate Immunity Database (IIID): an annotation tool for identifying immune genes in insect genomes. *PLoS One*. 2012; 7: e45125. <https://doi.org/10.1371/journal.pone.0045125> PMID: 22984621
44. Li L, Stoeckert CJ, Roos DS. OrthoMCL: identification of ortholog groups for eukaryotic genomes. *Genome Res*. 2003; 13: 2178–2189. <https://doi.org/10.1101/gr.1224503> PMID: 12952885
45. Waterhouse RM, Kriventseva EV, Meister S, Xi Z, Alvarez KS, Bartholomay LC, et al. Evolutionary dynamics of immune-related genes and pathways in disease-vector mosquitoes. *Science*. 2007; 316: 1738–1743. <https://doi.org/10.1126/science.1139862> PMID: 17588928
46. Yin C, Shen G, Guo D, Wang S, Ma X, Xiao H, et al. InsectBase: a resource for insect genomes and transcriptomes. *Nucleic Acids Res*. 2016; 44: D801–7. <https://doi.org/10.1093/nar/gkv1204> PMID: 26578584
47. Poelchau M, Childers C, Moore G, Tsavatapalli V, Evans J, Lee C-Y, et al. The i5k Workspace@NAL—enabling genomic data access, visualization and curation of arthropod genomes. *Nucleic Acids Res*. 2015; 43: D714–9. <https://doi.org/10.1093/nar/gku983> PMID: 25332403
48. Elsik CG, Tayal A, Diesh CM, Unni DR, Emery ML, Nguyen HN, et al. Hymenoptera Genome Database: integrating genome annotations in HymenopteraMine. *Nucleic Acids Res*. 2016; 44: D793–800. <https://doi.org/10.1093/nar/gkv1208> PMID: 26578564
49. Latorre-Estivalis JM, Robertson HM, Walden KKO, Ruiz J, Gonçalves LO, Guarneri AA, et al. The molecular sensory machinery of a Chagas disease vector: expression changes through imaginal moult and sexually dimorphic features. *Sci Rep*. 2017; 7: 40049. <https://doi.org/10.1038/srep40049> PMID: 28059141
50. Kumar S, Stecher G, Tamura K. MEGA7: molecular evolutionary genetics analysis version 7.0 for bigger datasets. *Mol Biol Evol*. 2016; 33: 1870–1874. <https://doi.org/10.1093/molbev/msw054> PMID: 27004904
51. Edgar RC. MUSCLE: multiple sequence alignment with high accuracy and high throughput. *Nucleic Acids Res*. 2004; 32: 1792–1797. <https://doi.org/10.1093/nar/gkh340> PMID: 15034147
52. Kanehisa M, Goto S. KEGG: kyoto encyclopedia of genes and genomes. *Nucleic Acids Res*. 2000; 28: 27–30. PMID: 10592173
53. Kersey PJ, Allen JE, Allot A, Barba M, Boddu S, Bolt BJ, et al. Ensembl Genomes 2018: an integrated omics infrastructure for non-vertebrate species. *Nucleic Acids Res*. 2018; 46: D802–D808. <https://doi.org/10.1093/nar/gkx1011> PMID: 29092050
54. Giraldo-Calderón GI, Emrich SJ, MacCallum RM, Maslen G, Dialynas E, Topalis P, et al. VectorBase: an updated bioinformatics resource for invertebrate vectors and other organisms related with human diseases. *Nucleic Acids Res*. 2015; 43: D707–13. <https://doi.org/10.1093/nar/gku1117> PMID: 25510499

55. Bottino-Rojas V, Talyuli OAC, Carrara L, Martins AJ, James AA, Oliveira PL, et al. The redox-sensing gene Nrf2 affects intestinal homeostasis, insecticide resistance, and Zika virus susceptibility in the mosquito *Aedes aegypti*. *J Biol Chem*. 2018; 293: 9053–9063. <https://doi.org/10.1074/jbc.RA117.001589> PMID: [29685890](https://pubmed.ncbi.nlm.nih.gov/29685890/)
56. Toubiana M, Rosani U, Giambelluca S, Cammarata M, Gerdol M, Pallavicini A, et al. Toll signal transduction pathway in bivalves: complete cds of intermediate elements and related gene transcription levels in hemocytes of immune stimulated *Mytilus galloprovincialis*. *Dev Comp Immunol*. 2014; 45: 300–312. <https://doi.org/10.1016/j.dci.2014.03.021> PMID: [24709052](https://pubmed.ncbi.nlm.nih.gov/24709052/)
57. Schmittgen TD, Livak KJ. Analyzing real-time PCR data by the comparative CT method. *Nat Protoc*. 2008; 3: 1101–1108. <https://doi.org/10.1038/nprot.2008.73> PMID: [18546601](https://pubmed.ncbi.nlm.nih.gov/18546601/)
58. Livak KJ, Schmittgen TD. Analysis of relative gene expression data using real-time quantitative PCR and the 2(-Delta Delta C(T)) Method. *Methods*. 2001; 25: 402–408. <https://doi.org/10.1006/meth.2001.1262> PMID: [11846609](https://pubmed.ncbi.nlm.nih.gov/11846609/)
59. Zumaya-Estrada FA, Martínez-Barnetche J, Lavore A, Rivera-Pomar R, Rodríguez MH. Comparative genomics analysis of triatomines reveals common first line and inducible immunity-related genes and the absence of Imd canonical components among hemimetabolous arthropods. *Parasit Vectors*. 2018; 11: 48. <https://doi.org/10.1186/s13071-017-2561-2> PMID: [29357911](https://pubmed.ncbi.nlm.nih.gov/29357911/)
60. Armisen D, Rajakumar R, Friedrich M, Benoit JB, Robertson HM, Panfilio KA, et al. The genome of the water strider *Gerris buenoi* reveals expansions of gene repertoires associated with adaptations to life on the water. *BioRxiv*. 2018; <https://doi.org/10.1101/242230>
61. Stanke M, Morgenstern B. AUGUSTUS: a web server for gene prediction in eukaryotes that allows user-defined constraints. *Nucleic Acids Res*. 2005; 33: W465–7. <https://doi.org/10.1093/nar/gki458> PMID: [15980513](https://pubmed.ncbi.nlm.nih.gov/15980513/)
62. Campbell MS, Holt C, Moore B, Yandell M. Genome Annotation and Curation Using MAKER and MAKER-P. *Curr Protoc Bioinformatics*. 2014; 48: 4.11.1–39. <https://doi.org/10.1002/0471250953.bi0411s48> PMID: [25501943](https://pubmed.ncbi.nlm.nih.gov/25501943/)
63. Oliva Chávez AS, Shaw DK, Munderloh UG, Pedra JHF. Tick humoral responses: marching to the beat of a different drummer. *Front Microbiol*. 2017; 8: 223. <https://doi.org/10.3389/fmicb.2017.00223> PMID: [28261180](https://pubmed.ncbi.nlm.nih.gov/28261180/)
64. Panfilio KA, Vargas Jentzsch IM, Benoit JB, Erezyilmaz D, Suzuki Y, Colella S, et al. Molecular evolutionary trends and feeding ecology diversification in the Hemiptera, anchored by the milkweed bug genome. *BioRxiv*. 2017; <https://doi.org/10.1101/201731>
65. Saha S, Hosmani PS, Villalobos-Ayala K, Miller S, Shippy T, Rosendale A, et al. Improved annotation of the insect vector of Citrus greening disease: Biocuration by a diverse genomics community. *BioRxiv*. 2017; <https://doi.org/10.1101/099168>
66. Arp AP, Hunter WB, Pelz-Stelinski KS. Annotation of the asian citrus psyllid genome reveals a reduced innate immune system. *Front Physiol*. 2016; 7: 570. <https://doi.org/10.3389/fphys.2016.00570> PMID: [27965582](https://pubmed.ncbi.nlm.nih.gov/27965582/)
67. Ioannidis P, Lu Y, Kumar N, Creasy T, Daugherty S, Chibucos MC, et al. Rapid transcriptome sequencing of an invasive pest, the brown marmorated stink bug *Halyomorpha halys*. *BMC Genomics*. 2014; 15: 738. <https://doi.org/10.1186/1471-2164-15-738> PMID: [25168586](https://pubmed.ncbi.nlm.nih.gov/25168586/)
68. Sloan DB, Nakabachi A, Richards S, Qu J, Murali SC, Gibbs RA, et al. Parallel histories of horizontal gene transfer facilitated extreme reduction of endosymbiont genomes in sap-feeding insects. *Mol Biol Evol*. 2014; 31: 857–871. <https://doi.org/10.1093/molbev/msu004> PMID: [24398322](https://pubmed.ncbi.nlm.nih.gov/24398322/)
69. Rao Q, Rollat-Farnier P-A, Zhu D-T, Santos-Garcia D, Silva FJ, Moya A, et al. Genome reduction and potential metabolic complementation of the dual endosymbionts in the whitefly *Bemisia tabaci*. *BMC Genomics*. 2015; 16: 226. <https://doi.org/10.1186/s12864-015-1379-6> PMID: [25887812](https://pubmed.ncbi.nlm.nih.gov/25887812/)
70. Song N, Liang A-P, Bu C-P. A molecular phylogeny of Hemiptera inferred from mitochondrial genome sequences. *PLoS One*. 2012; 7: e48778. <https://doi.org/10.1371/journal.pone.0048778> PMID: [23144967](https://pubmed.ncbi.nlm.nih.gov/23144967/)
71. Behrman EL, Howick VM, Kapun M, Staubach F, Bergland AO, Petrov DA, et al. Rapid seasonal evolution in innate immunity of wild *Drosophila melanogaster*. *Proc Biol Sci*. 2018; 285. <https://doi.org/10.1098/rspb.2017.2599> PMID: [29321302](https://pubmed.ncbi.nlm.nih.gov/29321302/)
72. McTaggart SJ, Obbard DJ, Conlon C, Little TJ. Immune genes undergo more adaptive evolution than non-immune system genes in *Daphnia pulex*. *BMC Evol Biol*. 2012; 12: 63. <https://doi.org/10.1186/1471-2148-12-63> PMID: [22577801](https://pubmed.ncbi.nlm.nih.gov/22577801/)
73. Lai AG, Aboobaker A. The innate immune systems of malacostracan crustaceans exhibit both conserved and evolutionarily distinct components. *BioRxiv*. 2016; <https://doi.org/10.1101/091835>

74. Obbard DJ, Welch JJ, Kim K-W, Jiggins FM. Quantifying adaptive evolution in the *Drosophila* immune system. *PLoS Genet.* 2009; 5: e1000698. <https://doi.org/10.1371/journal.pgen.1000698> PMID: [19851448](https://pubmed.ncbi.nlm.nih.gov/19851448/)
75. Han M, Qin S, Song X, Li Y, Jin P, Chen L, et al. Evolutionary rate patterns of genes involved in the *Drosophila* Toll and Imd signaling pathway. *BMC Evol Biol.* 2013; 13: 245. <https://doi.org/10.1186/1471-2148-13-245> PMID: [24209511](https://pubmed.ncbi.nlm.nih.gov/24209511/)
76. Sackton TB, Lazzaro BP, Schlenke TA, Evans JD, Hultmark D, Clark AG. Dynamic evolution of the innate immune system in *Drosophila*. *Nat Genet.* 2007; 39: 1461–1468. <https://doi.org/10.1038/ng.2007.60> PMID: [17987029](https://pubmed.ncbi.nlm.nih.gov/17987029/)
77. Bulmer MS, Crozier RH. Variation in positive selection in termite GNBPs and Relish. *Mol Biol Evol.* 2006; 23: 317–326. <https://doi.org/10.1093/molbev/msj037> PMID: [16221893](https://pubmed.ncbi.nlm.nih.gov/16221893/)
78. Begun DJ, Whitley P. Adaptive evolution of relish, a *Drosophila* NF-kappaB/IkappaB protein. *Genetics.* 2000; 154: 1231–1238. PMID: [10757765](https://pubmed.ncbi.nlm.nih.gov/10757765/)
79. Gordon ERL, McFrederick Q, Weirauch C. Phylogenetic evidence for ancient and persistent environmental symbiont reacquisition in largidae (hemiptera: heteroptera). *Appl Environ Microbiol.* 2016; 82: 7123–7133. <https://doi.org/10.1128/AEM.02114-16> PMID: [27694238](https://pubmed.ncbi.nlm.nih.gov/27694238/)
80. Toenshoff ER, Gruber D, Horn M. Co-evolution and symbiont replacement shaped the symbiosis between adelgids (Hemiptera: Adelgidae) and their bacterial symbionts. *Environ Microbiol.* 2012; 14: 1284–1295. <https://doi.org/10.1111/j.1462-2920.2012.02712.x> PMID: [22364314](https://pubmed.ncbi.nlm.nih.gov/22364314/)
81. Kuechler SM, Dettner K, Kehl S. Characterization of an obligate intracellular bacterium in the midgut epithelium of the bulrush bug *Chilacis typhae* (Heteroptera, Lygaeidae, Artheneinae). *Appl Environ Microbiol.* 2011; 77: 2869–2876. <https://doi.org/10.1128/AEM.02983-10> PMID: [21378044](https://pubmed.ncbi.nlm.nih.gov/21378044/)
82. Gerardo NM, Altincicek B, Anselme C, Atamian H, Barribeau SM, de Vos M, et al. Immunity and other defenses in pea aphids, *Acyrtosiphon pisum*. *Genome Biol.* 2010; 11: R21. <https://doi.org/10.1186/gb-2010-11-2-r21> PMID: [20178569](https://pubmed.ncbi.nlm.nih.gov/20178569/)
83. Díaz-Albiter HM, Ferreira TN, Costa SG, Rivas GB, Gumiel M, Cavalcante DR, et al. Everybody loves sugar: first report of plant feeding in triatomines. *Parasit Vectors.* 2016; 9: 114. <https://doi.org/10.1186/s13071-016-1401-0> PMID: [26928036](https://pubmed.ncbi.nlm.nih.gov/26928036/)
84. Alves CL, Araujo RN, Gontijo NF, Pereira MH. Importance and physiological effects of hemolymphagy in triatomines (Hemiptera: Reduviidae). *J Med Entomol.* 2011; 48: 372–381. <https://doi.org/10.1603/ME10151> PMID: [21485376](https://pubmed.ncbi.nlm.nih.gov/21485376/)
85. Noireau F, Diosque P, Jansen AM. *Trypanosoma cruzi*: adaptation to its vectors and its hosts. *Vet Res.* 2009; 40: 26. <https://doi.org/10.1051/vetres/2009009> PMID: [19250627](https://pubmed.ncbi.nlm.nih.gov/19250627/)
86. Wang J, Wu Y, Yang G, Aksoy S. Interactions between mutualist *Wigglesworthia* and tsetse peptidoglycan recognition protein (PGRP-LB) influence trypanosome transmission. *Proc Natl Acad Sci USA.* 2009; 106: 12133–12138. <https://doi.org/10.1073/pnas.0901226106> PMID: [19587241](https://pubmed.ncbi.nlm.nih.gov/19587241/)
87. Anselme C, Vallier A, Balmand S, Fauvarque M-O, Heddi A. Host PGRP gene expression and bacterial release in endosymbiosis of the weevil *Sitophilus zeamais*. *Appl Environ Microbiol.* 2006; 72: 6766–6772. <https://doi.org/10.1128/AEM.00942-06> PMID: [17021229](https://pubmed.ncbi.nlm.nih.gov/17021229/)
88. Zhang R, Zhu Y, Pang X, Xiao X, Zhang R, Cheng G. Regulation of Antimicrobial Peptides in *Aedes aegypti* Aag2 Cells. *Front Cell Infect Microbiol.* 2017; 7: 22. <https://doi.org/10.3389/fcimb.2017.00022> PMID: [28217557](https://pubmed.ncbi.nlm.nih.gov/28217557/)
89. Tanji T, Yun E-Y, Ip YT. Heterodimers of NF-kappaB transcription factors DIF and Relish regulate antimicrobial peptide genes in *Drosophila*. *Proc Natl Acad Sci USA.* 2010; 107: 14715–14720. <https://doi.org/10.1073/pnas.1009473107> PMID: [20679214](https://pubmed.ncbi.nlm.nih.gov/20679214/)
90. Zhong X, Rao X-J, Yi H-Y, Lin X-Y, Huang X-H, Yu X-Q. Co-expression of Dorsal and Rel2 Negatively Regulates Antimicrobial Peptide Expression in the Tobacco Hornworm *Manduca sexta*. *Sci Rep.* 2016; 6: 20654. <https://doi.org/10.1038/srep20654> PMID: [26847920](https://pubmed.ncbi.nlm.nih.gov/26847920/)